Report 2025

Title: AI-Powered 3D Sensors for Monitoring NPK Dynamics in Corn for Precision Fertilizer Management

Principal Investigators (PI): Azahar Ali

Principal Investigators (PI) Mailing Address (Street/ P.O. Box, City, State, Zip)

Food Science and Technology Building, Room 103
360 Duck Pond Drive
Blacksburg, VA 24061

Principal Investigators (PI) Email address: azahar@vt.edu

Report till December 2025

Objective

The objective of this phase of the project is the validation of plant-implantable NPK sensors in corn plants under greenhouse and field conditions. This work focuses on evaluating the performance, accuracy, and reliability of the developed sensors for real-time, in situ monitoring of nitrogen (N), phosphorus (P), and potassium (K) uptake in corn plants. Validation activities include sensor implantation into corn stalks, continuous monitoring of nutrient signals, comparison with reference nutrient analyses, assessment of matrix effects using corn sap, and evaluation of sensor stability and robustness under biologically relevant conditions.

Overall Status

During the 2025 project cycle, we successfully advanced the validation of the plant-implantable NPK sensing platform. The sensors demonstrated robust electrochemical performance, good selectivity and reproducibility, and were successfully integrated with a compact, battery-powered readout circuit enabling wireless data transmission. Initial greenhouse testing and proof-of-concept field deployments confirmed system readiness for expanded validation.

To support validation activities, corn sap samples were collected from BlackMarsh Farm, and corn plants were established in the Virginia Tech greenhouse for controlled studies. These greenhouse plants are being grown under defined nutrient treatments, including nitrate fertilizer, poultry litter, and manure, to replicate agronomically relevant nutrient conditions.

In parallel, a field-deployable readout and data transmission circuit was developed and integrated with the implantable sensors to enable continuous, real-time data collection. Ongoing work in the second half of the current funding cycle includes deploying the NPK sensors in greenhouse-grown corn plants and validating sensor outputs against bench-top measurements using collected corn sap to assess accuracy and matrix effects.

Building on these controlled validation studies, the project is on track for full in-field deployment in summer 2026. During this phase, plant-implantable sensors will be installed in corn fields and operated continuously for approximately one month to complete field-scale validation of the sensing platform.

Outcome: Below outcomes demonstrate successful technical validation, translational potential, and positioning of the technology for broader adoption and federal-scale funding

Peer-Reviewed Conference Proceeding

1. Ataei Kachouei, M., S. Chick, and Md. Azahar Ali*. 2025. *3D-Printed Plant-Implantable Sensor for Phosphate Detection in Corn*. In **Proceedings of the IEEE 7th International Conference on Emerging Electronics (IEEE-ICEE)** (accepted, in press).

Manuscript Under Preparation

- One additional research article on plant-implantable NPK sensing is currently under preparation for journal submission.

Intellectual Property

- **Virginia Tech Intellectual Properties (VTIP) Disclosure:**
  Ali, A., and M. Ataei Kachouei. *Implantable 3D-Printed Plant Sensors: Continuous Assessment of Nutrient Measurements in Corn Fields*. Tech ID: **25-076 (INV2025-065)**, filed in 2024.

External Funding Proposal

- Ali, A. (PI). 2025. *Storm-Aware Nutrient Management in Corn: Closing the Soil–Plant–Stormwater Loop*. Submitted to the **USDA–NIFA AFRI Competitive Grants Program, Foundational and Applied Science Program** (Engineering for Precision Crop and Water Management, **A1551**).

Representative Preliminary Results

1. System Overview and Validation Framework: Representative preliminary sensor results obtained to date demonstrate the feasibility, robustness, and validation readiness of the plant-implantable NPK sensing platform. The overall concept and validation framework are illustrated in Figure 1. The system employs needle-shaped, 3D-printed sensors for direct implantation into corn stalks, enabling real-time, in situ monitoring of nutrient uptake. Characteristic phosphorus (P), nitrogen (N), and potassium (K) deficiency signatures across corn growth stages highlight the agronomic relevance of continuous sensing. Validation is being conducted under greenhouse and field conditions across different fertilizer management practices, including commercial fertilizer, poultry litter, and manure.

2. Sensor Design, Fabrication, and System Integration: Figure 2 summarizes the design, fabrication, and system-level integration of the plant-implantable NPK sensor platform. The sensor features a needle-shaped, multi-electrode architecture optimized for minimally invasive insertion into corn stalks while maintaining mechanical robustness. Scanning electron microscopy (SEM) images confirm the formation of a sharp needle tip and uniform microstructured sensing surfaces with consistent feature spacing, supporting reproducible electrochemical performance.

To enable practical deployment, a compact, field-deployable readout circuit was developed for real-time signal acquisition. The integrated electronics support continuous data collection and wireless interfacing, enabling long-term monitoring under greenhouse and field conditions. Together, these results demonstrate successful sensor fabrication, structural integrity, and system readiness for in-plant validation studies.

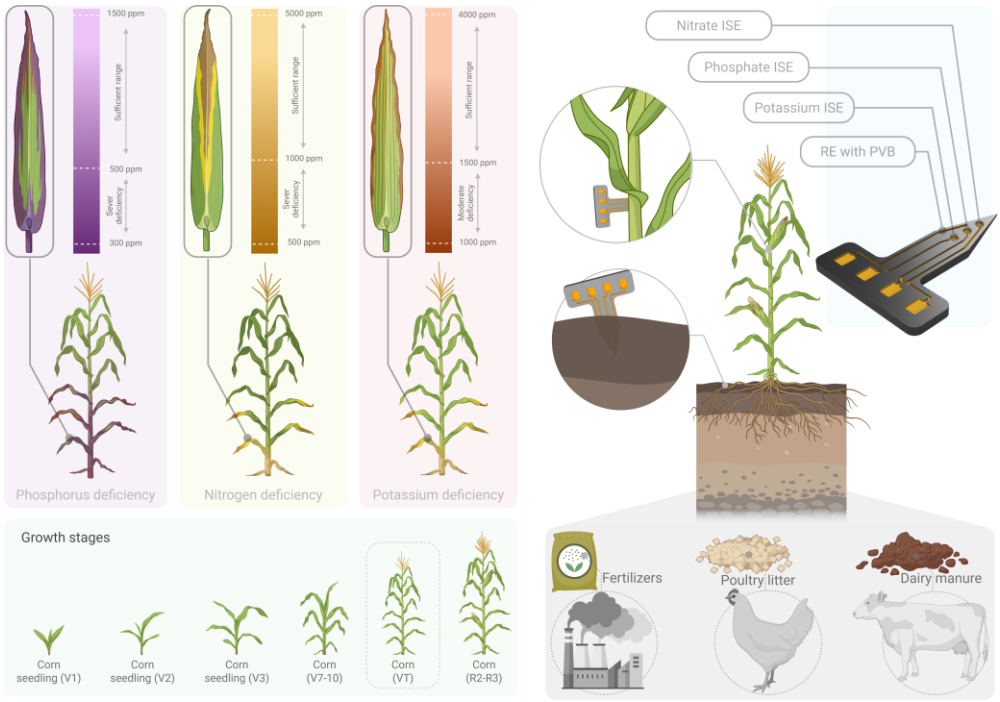

Figure 1. Plant-implantable NPK sensor concept and validation framework. This figure illustrates the deployment and validation of needle-shaped, 3D-printed NPK sensors for in situ monitoring of nutrient uptake in corn plants. Nutrient deficiency signatures for phosphorus, nitrogen, and potassium across growth stages are shown to highlight the agronomic relevance of continuous sensing. The schematic depicts direct sensor implantation into corn stalks with integrated readout circuitry for real-time data acquisition. Validation is performed under greenhouse and field conditions across different fertilizer treatments, including commercial fertilizer, poultry litter, and manure.

Phosphate sensor performance:

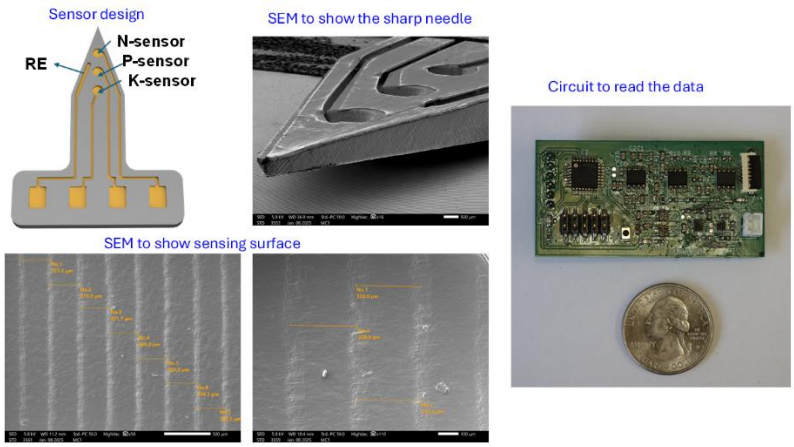

Figure 2. Design, fabrication, and system integration of the plant-implantable NPK sensor. Schematic of the needle-shaped sensor design, SEM images showing the sharp implantable needle tip and microstructured sensing surface, and a field-deployable readout circuit developed for real-time data acquisition from implanted sensors.

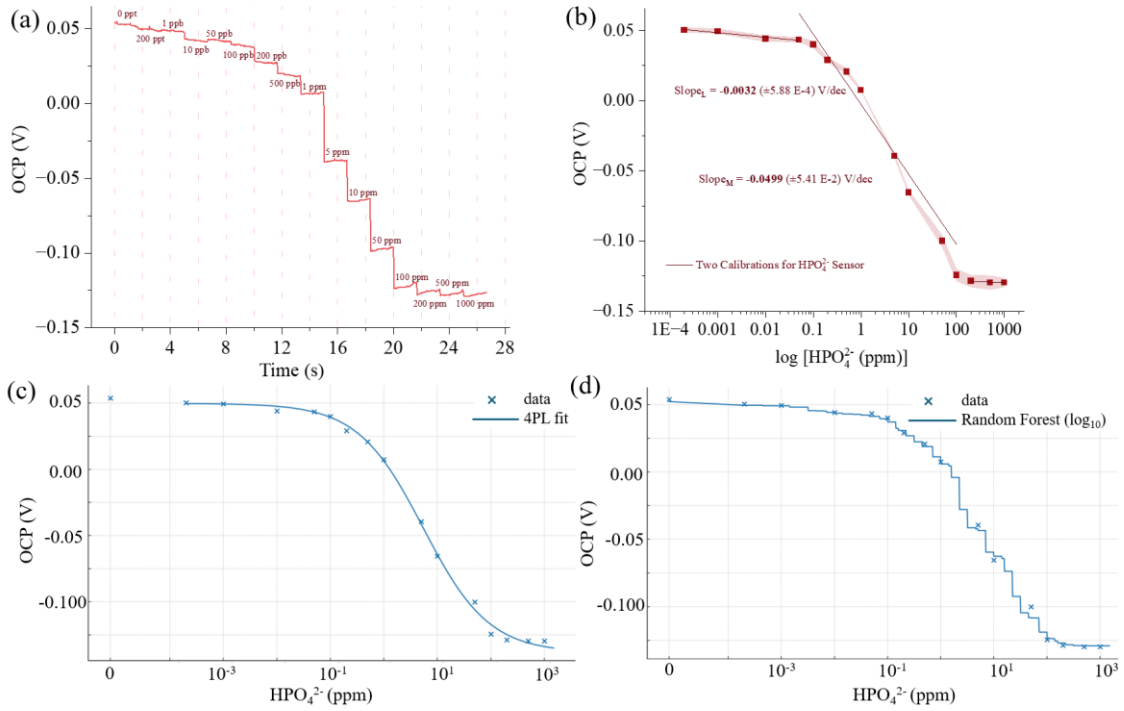

Figure 4. Sensing results. a) Open circuit potentiogram (OCP) of the phosphorus (P) sensor tested with standard HPO_4^{2-} solutions ranging from 200 ppt to 1000 ppm. Each concentration was measured for 100 s before immediately switching to the next solution. b) Calibration curve of the P sensor, showing two distinct sensitivity regions at low and intermediate HPO_4^{2-} concentrations. c) 4-parameter logistic (4PL) calibration. OCP (V) vs. phosphate (ppm; log x) with 4PL fit (top ≈ 0.0497 V, bottom ≈ −0.138 V, EC_{50} ≈ 5.48 ppm, h ≈ 0.71). Primary calibration; LOOCV RMSE ≈ 4.4 mV, d) Random Forest calibration (log_{10} features). OCP (V) vs. phosphate (ppm; log x) with RF fit (400 trees). Non-parametric check of the 4PL; LOOCV RMSE ≈ 7.4 mV.

3. Phosphate (P) Sensor Performance

3.1 Potentiometric Sensing and Calibration: The phosphate sensor operates based on potentiometric detection, measuring the open-circuit potential (OCP) between a phosphate-selective working electrode and a reference electrode under zero-current conditions. The phosphate-selective membrane generates a potential proportional to the logarithm of HPO_4^{2-} activity, resulting in staircase-like OCP responses during sequential concentration changes.

Figure 4 presents the phosphate sensor calibration results. The sensor exhibited clear potentiometric behavior over a wide concentration range from 200 ppt to 1000 ppm. Time-dependent OCP measurements showed rapid stabilization (~100 s) at each concentration step, confirming suitability for real-time monitoring. Two sensitivity regimes were observed: a low-sensitivity region at ppt–ppb concentrations and a near-Nernstian response in the mid-concentration range (0.01–200 ppm) with a slope of approximately −50 mV/dec. At higher concentrations (>200 ppm), the response plateaued, indicating membrane saturation.

3.2 Advanced Calibration and Modeling: To address nonlinear and saturating responses, calibration data were modeled using a four-parameter logistic (4PL) model and a Random Forest

(RF) regression approach. The 4PL model provided a smooth sigmoidal fit across the full dynamic range, with strong generalization performance (LOOCV RMSE ≈ 4.4 mV) and a reliable quantitative window of approximately 0.5–50 ppm. The estimated limit of detection (LOD) was 0.12–0.17 ppm, and the limit of quantification (LOQ) was 0.37–0.52 ppm.

As an independent, non-parametric validation, the Random Forest model reproduced the sigmoidal response with comparable accuracy (LOOCV RMSE ≈ 7.4 mV), corroborating the effective sensing range and supporting future applications such as drift correction and multi-sensor fusion.

3.3 Selectivity, Reproducibility, and Field Validation: Selectivity studies demonstrated stable phosphate sensing in the presence of common interfering ions. Calcium ions had negligible influence, while iron ions induced only a minor potential shift (~3–4 mV), confirming effective discrimination by the phosphate-selective membrane. Reproducibility assessments using independently fabricated sensors showed consistent OCP responses with a relative standard deviation of approximately ±6%, confirming fabrication reliability. Proof-of-concept field deployment at the BlackMarsh corn farm (Fredericksburg, VA) demonstrated stable sensor operation when directly interfaced with corn stalks, validating feasibility for in situ phosphate monitoring under real agricultural conditions. Ongoing studies are extending these tests to diverse fertilizer inputs and application rates.

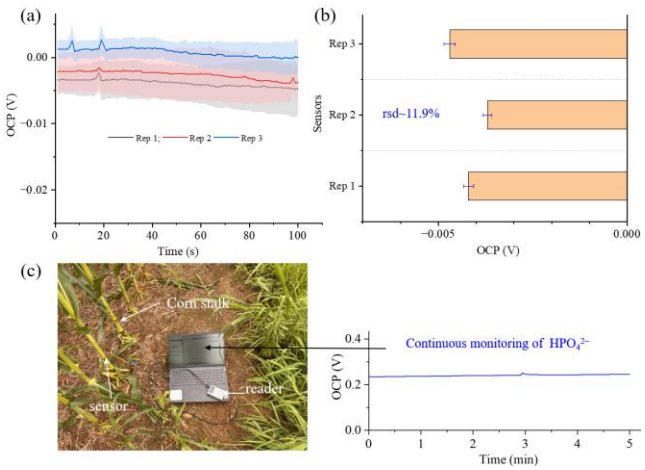

Figure 5. Reproducibility studies. a) OCP of the P sensor measurements that independently repeated five times with the same solution of 50 ppm HPO_4^{2-}. Each test was repeated three times, with the shaded area representing standard deviation. b) Repeatability assessment of the P sensor using repeated measurements in the same solution, yielding an RSD of ±6%. c) A proof of concept demonstrating continuous in-field monitoring via a sensor interfaced to corn plants. The P-sensor was used to monitor HPO_4^{2-} for 5 min continuously.

4. Potassium (K^+) Sensor Performance

The potassium sensor exhibited clear stepwise OCP responses to increasing K^+ concentrations ranging from 1 to 4000 ppm, with rapid stabilization suitable for real-time monitoring. Calibration

showed a strong linear relationship between OCP and log[K^+], with a near-Nernstian slope of 0.047 V/dec and a high correlation coefficient (Pearson's r = 0.99).
Repeatability testing yielded an RSD of 5.52%, confirming stable and reproducible performance. Selectivity studies demonstrated robust discrimination against common interfering ions, including Ca^{2+}, Fe^{2+}/Fe^{3+}, Mg^{2+}, HPO_4^{2-}, and NO_3^- ($p < 0.0001$). These results confirm the suitability of the K^+ sensor for in situ potassium monitoring in plant and field environments.

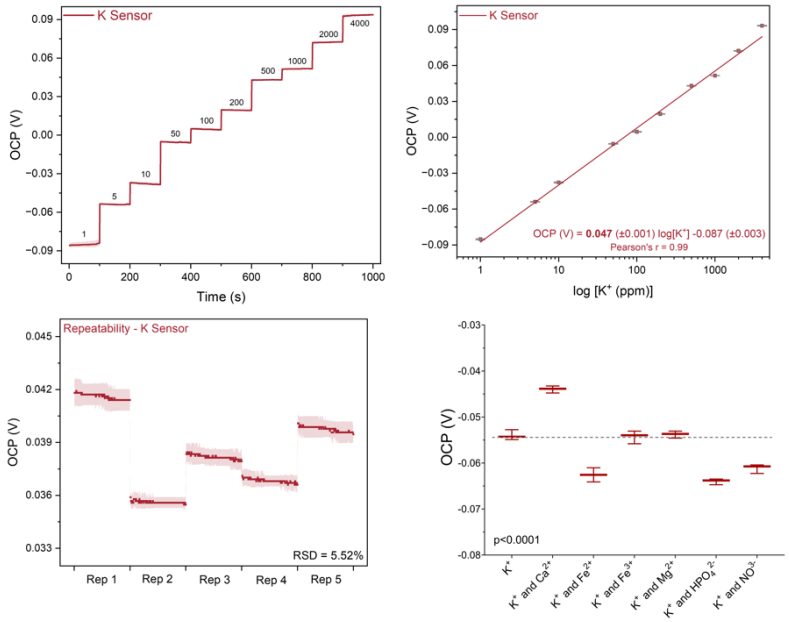

Figure 6. Electrochemical performance of the plant-implantable potassium (K^+) sensor. Time-resolved OCP response to increasing K^+ concentrations, calibration curve showing near-Nernstian sensitivity, repeatability across independent measurements, and selectivity in the presence of common interfering ions.

5. Nitrate (N) Sensor Performance

The nitrate sensor demonstrated reliable detection across a wide concentration range from 1 to 1200 ppm, with sensitivity down to 1 ppm. The sensor exhibited an inverse relationship between OCP and nitrate concentration, consistent with potentiometric nitrate sensing principles. High selectivity was achieved using a nitrate-selective membrane, with minimal interference from K^+, Na^+, and Cl^- ions.

To evaluate quantitative performance, sensor data were modeled using multiple machine-learning approaches. The Random Forest model provided the highest predictive accuracy ($r^2 = 0.87$, MSE = 0.00089), followed by Polynomial Regression ($r^2 = 0.79$). Linear Regression and SVM showed moderate performance, while the Decision Tree model was less effective. These results confirm the N-sensor's broad dynamic range, good selectivity, and robust predictive capability.

6. Deployment and Validation Readiness

Figure 7 demonstrates practical deployment of the plant-implantable NPK sensors under controlled and semi-field conditions, including direct attachment to corn stalks, greenhouse validation with potted plants, and implantation in soil-grown corn. These demonstrations highlight the mechanical robustness, ease of deployment, and readiness of the sensing platform for expanded field-scale validation

Figure 7. Deployment of plant-implantable NPK sensors in corn. Representative images showing sensor attachment to corn stalks, greenhouse-based validation with potted corn plants, and direct implantation in soil-grown corn, demonstrating readiness for in situ and field deployment.

Circuit Design and Data Transmission

The voltage signal generated by the plant-implantable sensor must be accurately measured and transmitted to the end user. Figure 8 presents the block diagram of the measurement and transmission system. The circuit is composed of three main functional sections: (1) signal conditioning, (2) data acquisition and transmission, and (3) power management. Each subsystem is designed to ensure accurate, low-noise signal processing and reliable operation under field conditions. The complete developed circuit is shown in Figure 2.

Signal Conditioning: The native output range of the sensor spans approximately −400 mV to +400 mV, whereas the input range of the microcontroller unit (MCU) analog-to-digital converter (ADC) is limited to 0–5 V. Directly interfacing the sensor output with the MCU would therefore result in signal clipping and data loss. To address this mismatch, a dedicated signal-conditioning stage was implemented, as shown in Figure 9.

A differential amplifier is used to amplify the voltage difference between the sensor electrodes. An appropriate DC offset is then applied to shift the signal into the measurable range of the MCU ADC. Two stages of analog filtering are incorporated to suppress high-frequency noise and improve signal stability. After amplification, offset adjustment, and filtering, the conditioned analog signal is suitable for accurate digitization by the MCU.

Data Acquisition and Transmission: An ATmega328 microcontroller was used for data acquisition and processing due to its low power consumption and suitability for battery-operated systems. The conditioned sensor signal is digitized using the MCU's internal 10-bit ADC and subsequently processed for wireless transmission. A Bluetooth module is integrated for data communication, allowing users to connect to the system via a mobile device. Sensor data are transmitted in real time to a Bluetooth terminal application on a smartphone, enabling remote monitoring and visualization.

Power Management: The circuit is powered by a 3.7 V lithium-ion battery, which supplies both the analog and digital subsystems. As illustrated in Figure 10, the battery voltage is first boosted to 5 V using a DC–DC boost converter. From this regulated 5 V rail, additional supply lines are generated to power the signal-conditioning circuitry, ADC, MCU, and Bluetooth module.

Separate regulation of analog and digital power domains was implemented to minimize noise coupling from digital components (MCU and Bluetooth module) into the sensitive analog front-end. This power management strategy ensures stable operation and reliable signal integrity during continuous sensing and wireless data transmission in greenhouse and field environments.

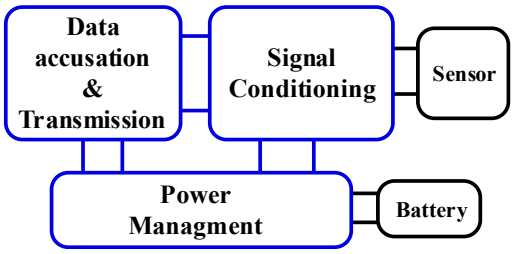

Fig. 8: block diagram of the measurement system

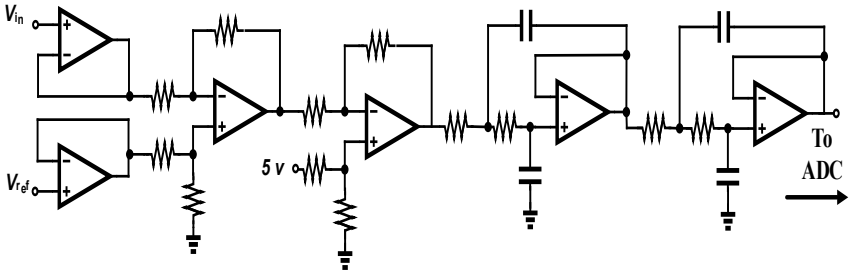

Fig. 9: Schematic of the circuit

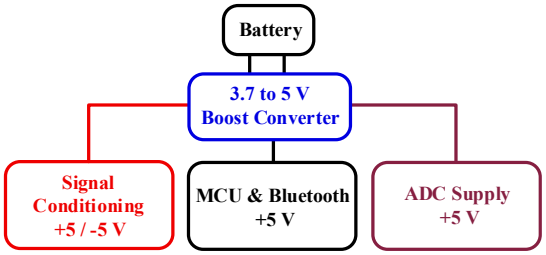

Fig. 10: Supply distribution diagram.

Short Summary of Progress to Date

We have successfully developed and preliminarily validated a 3D-printed, plant-implantable NPK sensing platform for real-time, in situ monitoring of nutrient uptake in corn. The sensors demonstrated robust electrochemical performance, good selectivity and reproducibility, and were successfully integrated with a compact, battery-powered readout and wireless data transmission system. Initial greenhouse and proof-of-concept field deployments confirm system readiness for expanded field-scale validation.

Next Steps (Within the Current Funding Cycle)

To complete the objective of in-field sensor validation, we are growing corn in the Virginia Tech greenhouse under controlled nutrient treatments, including nitrate fertilizer, poultry litter, and manure. Plant-implantable NPK sensors will be deployed in these plants along with the developed readout circuitry to enable continuous, real-time data collection. Sensor outputs will be validated against bench-top measurements using collected corn sap to assess accuracy and matrix effects. Building on these results, full in-field deployment will be conducted in summer 2026, with sensors installed in corn fields to collect continuous nutrient uptake data over an extended period (~one month), completing field-scale validation of the sensing platform.